

I.O.S.

**SENSORS FOR THE MEASUREMENT OF THE
TRANSPORT OF SAND AS BEDLOAD**

by

A P SALKIELD

**A survey of requirements and possibilities
for development**

Report No 73

1978

**NATURAL ENVIRONMENT
INSTITUTE OF OCEANOGRAPHIC
SCIENCES
RESEARCH COUNCIL**

INSTITUTE OF OCEANOGRAPHIC SCIENCES

Wormley, Godalming,
Surrey, GU8 5UB.
(0428 - 79 - 4141)

(Director: Dr. A.S. Laughton)

Bidston Observatory,
Birkenhead,
Merseyside, L43 7RA.
(051 - 653 - 8633)

(Assistant Director: Dr. D.E. Cartwright)

Crossway,
Taunton,
Somerset, TA1 2DW.
(0823 - 86211)

(Assistant Director: M.J. Tucker)

*On citing this report in a bibliography the reference should be followed by
the words UNPUBLISHED MANUSCRIPT.*

SENSORS FOR THE MEASUREMENT OF THE
TRANSPORT OF SAND AS BEDLOAD

by

A P SALKIELD

A survey of requirements and possibilities
for development

Report No 73

1978

Institute of Oceanographic Sciences
Crossway
Taunton, Somerset, UK

CONTENTS

	Page
ABSTRACT	1
1 DEFINITION OF THE PROBLEM	1
1.1 Introduction	1
1.2 Characteristics of Bedload Movement	2
1.3 Summary of design constraints	7
2 REVIEW OF MEASUREMENT TECHNIQUES	8
2.1 Existing Instruments	8
2.2 Comments of existing methods	9
2.3 Techniques suitable for development	9
3 CONCLUSIONS	12
ACKNOWLEDGEMENTS	13
APPENDIX A - Self generated noise	14
APPENDIX B - Acoustic doppler	20
REFERENCES	29
FIGURES	

ABSTRACT

A study is made of the requirements of sensors for the measurement of the bedload transport of sand. The characteristics of bedload movement are examined in sufficient detail to enable the specification of the design requirements of suitable instruments. Three possible techniques suitable for development are discussed:

- (1) Self-generated noise
- (2) Acoustic Doppler and Backscatter Concentration determination
- (3) Pit sampler with pumped extraction

No individual instrument satisfies the design specification completely and the combined use of the promising instruments is proposed.

1. DEFINITION OF THE PROBLEM

1.1 Introduction

This report is a companion to IOS Report No 27/1977 (SOULSBY, 1977) which surveyed the instrumentation requirements for the measurement of suspended load transport. It also contained a brief review of the development of sedimentation instrumentation within IOS, and therefore no historical background information is included in this introduction.

Sand is transported as bedload when the stress exerted by the flow is large enough to produce movement, but not suspension of the sediment particles. If a rigorous definition is adopted, the sand is supported solely by solid transmitted stress and moves by sliding or rolling.

Bedload movement near threshold is intermittent in both space and time, while at higher flow movement is more intense, exhibiting significant particle interaction which modifies the flow field and turbulence characteristics near the bed. Further increases of flow lead to concurrent suspension. This effect is gradual with no marked transition between bedload and suspended transport. In both modes of transport a high gradient of sediment concentration and flow velocity occurs over the 10 cms or so near the bed.

Visual observations of bedload transport in the field are very dependent on the turbidity of the water column and in consequence are restricted in their scope. However, direct observations have been made on beaches and in shallow water where the motive power is primarily wave generated; and by underwater television and divers in deeper water, where tidal currents tend to predominate.

Experimental data obtained from rivers and laboratory flumes, gathered with traps and boxes, have enabled estimates of bedload transport rates to be made; however, very little reliable quantitative marine field data is available. The primary reason for this scarcity of data is the almost complete lack of suitable measurement techniques and instrumentation.

From the theoretical viewpoint many formulae for calculating bedload transport rates have been developed. The methods are varied, for example, EINSTEIN (1950) used a probabilistic method based on a statistical consideration of lift forces, BAGNOLD (1966) used physical arguments based on the concept of work done, and the theory of ACKERS and WHITE (1965) was developed through dimensional reasoning.

The equations all require determination of empirical constants, which are normally obtained from flume or river data. This factor tends to limit the application of a particular equation to the calculation of transport occurring under similar hydraulic and sedimentary conditions to those applying in the development of the equation. This limitation is particularly acute for marine applications because reliable transport data is sparse and comparison between the theories correspondingly difficult to make. The discrepancies between the equations may be quite wide particularly near the threshold of movement.

The estimates of transport rates used in this report to develop requirement specifications are made by using the method given by STERNBERG (1972). This is a modification of Bagnold's work and has been applied to transport problems in the marine field.

1.2 Characteristics of Bedload Movement

Initiation of grain movement: Considerable effort has been expended over the last two hundred years to formulate the conditions of incipient motion, resulting in numerous treatments and expressions. SHIELDS (1936) produced a widely accepted criterion based on experimental results, which is reproduced in dimensionalised form in Figure 1. The general trend of Shields' results have been confirmed by many other workers and for the purpose of this report review of the criterion is unnecessary.

Typical threshold values of u_* and u_{100} at four selected particle diameters are given in Table 1.

Table 1

Diameter μm		60	200	500	1000
u_{*c}	$cm s^{-1}$	1.40	1.45	1.70	2.40
u_{100}	$cm s^{-1}$	21	22	25	36

Threshold velocities for oscillatory flows under waves are of similar magnitude, although dependent on wave period. The reason for the dependence is probably that not only is the orbital velocity of importance, but also the value of the 'end of stroke' acceleration, which for the same orbital velocity, increases with decreasing wave period.

Forms of grain motion: The early concept of bed movement proposed by DU BOYS (1879) assumed that the fluid 'drags' a one grain diameter thick 'carpet' along the boundary, which in turn induces motion into the underlying layers, with the velocity of the layers decreasing in a linear manner.

Subsequent observations have demonstrated that this is not the case, and that modes of transport occur which are dependent on the transport stage, (defined as u_* / u_{*c}). FRANCIS (1973) describes laboratory experiments on solitary grains over a fixed bed in which three modes of transport were identified.

- (1) Rolling: This occurs at shear stresses near threshold, at a transport stage of approximately unity.
- (2) Saltation: As the shear stress increases the grains tend to move in a series of jumps which appear to result from momentary impulses caused by bed contacts. The trajectories are concave downwards and the maximum rise above the bed is 2 to 4 grain diameters.
- (3) Suspension: This occurs at higher transport stages, saltation appears to die out altogether at transport stages of about 2.2 and 5.5 for angular and rounded grains respectively.

The separation of transported material into 'bedload' and 'suspended load' is an idealisation. The transition between a saltation trajectory and a suspended path is not abrupt, and there is no distinct value of shear stress at which the transition occurs.

In the field situation the same modes of transport may be identified, with similar characteristics to those exhibited in the flume studies of Francis.

Effect of Topography: The experiments of Francis were limited by using single grains and a fixed bed, which prevented the normally spontaneously formed bed features, ripples, dunes etc, from appearing. Under natural conditions a fully mobile sediment bed deforms in stages, the normal sequence of these stages with increasing flow is as follows:

- (1) Threshold flat bed
- (2) Ripples
- (3) Dunes or megaripples
- (4) Transitional
- (5) Antidunes

These surface features move and change with alterations in the flow, but over the range of flow parameters that are normally encountered in the sea, ripples and dunes are the prevalent bed forms.

Bed features lead to form drag and a redistribution of the surface frictional stress, in such a way that sediment movement occurs in different modes on the various parts of the profile.

Ripples form when the flow is only slightly beyond the threshold of movement and the number of grains in motion is small. The particles move up the upstream or stoss slope by rolling or saltation and fall over the crest. This leads to a downstream translation of the form.

Some grains become separated from the crest and land approximately six ripple heights downstream. This reattachment point on the form exhibits zero mean shear and grains show a 'hesitancy' in movement, some grains moving forward, some backward (RAUDKIVI, 1967).

Under oscillatory flow when ripples are present, the character of the sediment motion in a layer of a thickness of the order of one or two times the ripple height largely differs from the motion in higher layers. In the lower layers the sediment is caught in the eddies on the leeside of the ripples; these eddies are swept over the ripples with the reversal in flow, after which the eddies weaken and some sand falls to the bed. The rest may be suspended for a period of time.

Bedforms also increase the variability of the areal distribution of movement. Ripples tend to form irregular patterns with many intersections: dune patterns are simpler with regular linear crest lines.

Typical dimensions of ripples and dunes are given below, though the total range may be very much greater.

TABLE 2

Bed feature	Amplitude cm	Wavelength m
Ripple	0.5 - 4	0.1 - 0.25
Dune (Megaripples)	5 - 15	0.5 - 3

In summary to this section, movement may occur over a range of areas, from the scale of an individual grain through ripples with mobile areas several square centimetres in extent, up to dune crest motion covering several square metres. Different modes of motion occur on the various parts of a bedform profile with a resultant spatial distribution in bedload velocity.

This range of both areal movement and velocity is a factor the effect of which must be considered on deployment techniques and on the sensing dimensions of any instrument.

Velocity of grain movement: Very little reliable data on the velocity of bedload movement is available. This comment applies to both flume investigations and marine field studies.

Therefore in this report an upper measurement limit for particle velocity of 30 cms^{-1} is proposed.

As stated earlier in the report, the region of interest in bedload transport is the bed, and the water column to a height of about 10cm above the bed. The velocity of grains moving as bedload is smaller than that of suspended grains, which may be assumed to be the same as the water velocity. Therefore, the maximum bedload velocity will be less than the water velocity at a height of 10 cm.

For a maximum u_{*} of 4.5 cms^{-1} and assuming a z_0 of 0.5 cm, a water velocity of about 34 cms^{-1} occurs at 10 cm (assuming a logarithmic profile).

Hence, it seems sensible to design for a maximum bedload velocity of 30 cms^{-1} but with a reasonable resolution; because the uppermost grains will be approaching the suspended velocity, while grains nearest the bed may be near threshold or at zero velocity. In between these extremes there will be an intermediate and unknown velocity distribution which is liable to be modified by the concentration of saltating particles.

Rate of Mass Transport: Although the rate of mass transport is not specifically required for instrument specification, such information is required later in the report and is included at this point.

In order to obtain representative values for the rate of mass transport Bagnold's theory as modified for marine application by STERNBERG (1972) is used. Bagnold's theory relates the mass transport rate to the available power expended by the flow on the boundary. This relationship is expressed as

$$g j_b \frac{\rho_s - \rho}{\rho_s} = K \omega$$

j_b = mass discharge of sediment
 ω = fluid power
 ϵ_b = efficiency factor
 $\tan \alpha$ = friction angle
 ρ_s = sediment density
 ρ = fluid density

where $K = \frac{\epsilon_b}{\tan \alpha}$

The field measurements of KACHEL and STERNBERG (1971) indicated that K is a function of the excess boundary shear stress ($\frac{\tau_0 - \tau_c}{\tau_c}$), and to provide empirical relationships between K , $\frac{\tau_0 - \tau_c}{\tau_c}$ and the mean sediment diameter, d , the flume data of GUY et al (1966) were analysed.

From the relationships obtained the bedload transport rate may be established under flow conditions and particle sizes for which the method is valid.

The limitations are as follows:

1. In a tidal current the flow conditions should be in an accelerating or a relatively steady part of the tidal cycle.
2. The technique is considered applicable for mean sediment sizes between approximately 200 μm and 2mm.
3. There should be little or no transport as suspended load.

Calculated bedload transport rates using the 'Sternberg method' for representative marine situations are given in Table 3.

TABLE 3

Sediment diameter d μm	$u_x = 2.5 \text{ cms}^{-1}$		$u_x = 3.5 \text{ cms}^{-1}$		$u_x = 4.5 \text{ cms}^{-1}$	
	$j_b \text{ kg m}^{-1} \text{ s}^{-1}$	$\frac{u_x}{u_{xc}}$	$j_b \text{ kg m}^{-1} \text{ s}^{-1}$	$\frac{u_x}{u_{xc}}$	$j_b \text{ kg m}^{-1} \text{ s}^{-1}$	$\frac{u_x}{u_{xc}}$
200	4.3×10^{-5}	1.72	7.7×10^{-4}	2.4	1.1×10^{-2}	3.1
500	6.1×10^{-5}	1.47	3.5×10^{-3}	2.05	2.0×10^{-1}	2.44
1000	2.0×10^{-5}	1.04	1.12×10^{-1}	1.46	1.54×10^0	1.90

Concentration Levels: Concentration levels occurring during bed-load transport are extremely variable in temporal and spatial distribution and in amplitude. The largest concentrations are present during avalanche movement on the lee slopes of ripple and 'sheet' flow on the top of dunes when influenced by wave action. The bed under these conditions flows as a fluid with a very high and nearly constant concentration, with a depth of movement of several grain diameters or more.

When movement occurs the sediment dilates, therefore the volume concentration will be less than the maximum possible. BAGNOLD (1955) suggests that a maximum volume concentration of 0.65 (831,000 ppm for quartz grains) is a realistic figure for natural reasonably rounded uniform grains and that shearing and movement should be possible at some value of volume concentration between 0.45 and 0.58 (684,000 and 785,000 ppm).

The concentration of moving material in a layer immediately above the bed may vary between zero and the concentration quoted above, but the extreme difficulty in measurement caused by the thinness of the bedload layer (2-4 grain diameters) and the space/time variability, has resulted in reliable field data not being available. However, data obtained by optical methods of concentrations of up to 150,000 ppm 'near' the bed under breaking waves have been reported by BRENNINKMEYER (1976) and up to 10,000 ppm under conditions of tidal flow by BHATTACHARYA et al (1969).

1.3 Summary of design constraints

The information presented in section 1.2 describes characteristics of bedload movement and transport necessary to specify the limiting criteria for any instrument.

The measurement requirement may be divided into two parts:

1. To detect the threshold of sediment movement; and
2. To provide quantitative data on bedload transport rates for sand sized sediments.

Instruments designed to satisfy the second requirement may prove suitable for the first, but not vice-versa, therefore it is preferable to concentrate on viable instruments of the second type.

The instrument should respond to sand grains in the size range $100\mu\text{m}$ to about 2 mm. (Grains smaller than approximately $100\mu\text{m}$ tend to move straight into suspension without an intermediate bedload stage). Concentrations in the saltation layer may range from zero to 150,000 ppm by weight, and volume

concentrations of approximately 0.5 (approximately 725,000 ppm) will be present during 'sheet flow'. The sensor should be able to resolve movement over an area of ten square centimetres or less. A range of velocity of particle movement of zero to 30 cms⁻¹ should be catered for.

The thickness of the bed load layer in which measurements are required is difficult to define, but will be of the order of 8 grain diameters in the saltation case, and about 4 grain diameters deep in the sheet flow situation. Therefore the active volume has to be relatively thin in the vertical.

The output of the instrument should be in a form suitable for continuous recording, and low power consumption to enable remote self recording would be advantageous.

2. REVIEW OF MEASUREMENT TECHNIQUES

2.1 Existing instruments

Reviews of early bed load measurement devices have been published by HUBBELL (1964) and by GRAF (1971). The apparatuses described are direct measurement devices which were lowered onto the bed and left in place for a known time interval. Detailed descriptions are also given in "Report 2: Equipment used for sampling Bed load and Bed material", of the FEDERAL INTERAGENCY RIVER BASIN COMMITTEE (1940), hence such devices are only mentioned briefly.

Direct samplers may be classified into one of the following types:

- (a) Box or basket samplers - a pervious container in which bedload accumulates;
- (b) Pan or tray samplers - sediment drops through slots into a buried container;
- (c) Pressure difference samplers - box samplers modified to reduce resistance to the flow;
- (d) Pit samplers - depressions in which sediment accumulates and is removed by pumping;
- (e) Pumped sampling - from a nozzle located in the bedload layer.

Indirect techniques that have been proposed and used may be classified as listed below:

- (a) Acoustic methods - three techniques have been reported:
 - (1) "Self-generated noise", in which acoustic energy produced by particle to particle impact is measured;
 - (2) Attenuation measurements based on scattering and absorption, and related to sediment concentration;
 - (3) The use of echo sounders to monitor bedform movement, from which bedload discharge may be calculated if certain assumptions are made.

- (b) Photographic - ripple migration has been measured photographically, and additional amplitude information obtained by stereophotogrammetry.

2.2 Comments on existing methods

None of the existing individual techniques provide completely reliable and quantitative data on bedload transport rates, and are limited by taking one-off samples, or integrating over a long time. Direct techniques have almost entirely been used in rivers where the particle size is larger than sand size range, but such samplers may be used to collect sand sized particles if the screen openings are sufficiently small.

The average efficiency of box and basket samplers is quoted at about 45% depending on particle size, bed discharge and the position of the sampler relative to bedforms. Such efficiencies are measured in flumes taking the total sand discharge as a reference, and the results may be subject to errors introduced by the influence of the sampler on water flow and the particle movement.

However, most indirect techniques are as yet at a stage of early development and as such unproven. Some form of direct sampling is the only technique available to provide control information. HUBBELL (1964), reports on several types of pit sampler and states on the basis of flume experiments that sampling efficiencies of almost 100% may be achieved. Providing the deficiencies of such samplers and the method of calibration are accepted, some development effort on direct sampling is warranted.

RICHARDSON et al (1961) monitored bedform movement with echo sounders and related the velocity of bedform translation to bedload discharge. The technique assumed a triangular profile in longitudinal section, which is rarely found in nature, and the method is most applicable to coarse-grained sediments with dune bedforms. The method is considered inapplicable in the context of this report.

The same conclusion applies to photographic techniques, which depend on large numbers of sequential photographs. These are difficult to obtain in low visibility estuarine and coastal environments and introduce long time delays between data gathering and analysis.

The techniques that are considered suitable for development are briefly discussed in the next section and in detail in the appendices.

2.3 Techniques suitable for development

Self-generated noise: Bands of noise have been observed on the records of high

frequency side scan sonars and also on sector scan sonar displays. These noise bands are coincident on the records with the position of sand wave crests at times of high water flow velocities. Sand movement occurring at the crests was thought to be the most likely source of the noise.

The idea of measurement of self-generated noise is not new, and noise data were obtained from the Danube as early as 1963 by BEDEUS and IVISICS and in a laboratory flume by JOHNSON and MUIR (1969). However application of the technique to the marine situation has not been reported.

In order to investigate the application of the technique in the sea, preliminary research was embarked on at IOS (Wormley). MILLARD (1976a) reported on the initial laboratory work, in which measurements of acoustic noise were taken in a submerged drum. This was usually rotated at a constant angular velocity about a horizontal axis through the ends of the drum. Sized sediment samples were placed in the drum and frequency spectra of the resultant noise were obtained. Figure 2 shows typical data.

The amplitude of the spectral peak for any particular sediment varied from sweep to sweep of the analyser, but occurred at approximately the same frequency. There was a shift to a higher frequency if the rotational rate of the drum was increased and an opposite effect on slowing down.

Initially it was assumed that the frequency dependence could be related to spherical harmonic vibrations of individual particles. However calculations indicate that frequencies in the megahertz region should be expected from particles in the sand size range. The mechanism producing the lower frequency peaks appears to be a particle interaction, in the simplest case with two particles forming a double mass system with a compliance acting at the point of contact. Figure 3 shows the expected theoretical frequency/interparticle force relationship for 2.7 cm diameter steel spheres, together with experimental results. A known force was applied between the spheres which were then excited with a small a.c. field to produce the measured vibration.

The nature and magnitude of interparticle forces in the case of sediment moving in the drum or in the marine situation is indeterminant. Figure 4 shows theoretical lines for forces of 0.01N, 1N and 100N, with superimposed experimental results for shingle and ballotini. The data are difficult to interpret but this may be a result of the particular experimental apparatus.

Subsequent field experiments, MILLARD (1976b) combining the measurement of self-generated noise and underwater television observation indicate that the frequency/particle size relationship observed in the field is similar to that

obtained in the laboratory drum experiments. Wave tank experiments have shown that it is possible to detect the movement of very small quantities of sand in an oscillatory flow.

These findings have been used by IOS to design a threshold indicating instrument for use under low amplitude wave conditions, when water velocities are close to threshold and movement occurs predominantly as bedload. This is at present under field evaluation.

The next stage of development hinges on obtaining an understandable relationship between bedload transport rate and a measure of the resultant noise. Relationships are calculated and discussed in Appendix A, but some general points are relevant at this juncture.

The technique is suited for use under a limited range of conditions, near to threshold and with material at the coarse end of the size range. This is an inevitable outcome from the noise generating mechanism, because as the transport stage increases with concurrent saltation and suspension, a saturation effect occurs. In the limit little noise will be generated if all the transport is by suspension.

Acoustic Doppler Techniques: Techniques developed in the medical field lend themselves to application to marine measurement problems, quantitative physiological information on blood flow velocity, velocity profile and blood vessel cross sectional area being currently obtained by ultrasonic doppler methods.

By the use of doppler techniques it should be possible to measure the velocity of particles moving in contact with the bed and the velocity profile within the 'saltation layer'. A similar technique also has obvious application to velocity determination of suspended sand at greater elevations above the bed.

Acoustic scattering measurements should also reveal information on particle concentration. However the practical situation is very complex. Surface back-scattering depends on a large number of variables including the acoustic wavelength/particle size ratio, gross surface roughness, inclination etc. The overall effect of these variables is that at oblique incidence the surface backscattering coefficient is not a sensitive measure of particle concentration. However, determination of bedload particle velocity in conjunction with self-generated noise data should produce valuable information on the transport of material in contact with the bed.

At higher flow stages or with finer material, when a 'saltation layer'

is developed, application of echo integration techniques on the doppler shifted volume backscattered signal should allow estimation of concentration to be made, concurrent with velocity determination. Range gating would allow such measurements to be made in range cells at chosen altitudes above the bed. As a prerequisite for such estimation of concentration, basic laboratory measurements are required on the target strengths of sand in water.

To obtain simultaneous spatial concentrations and velocity distributions, a pulsed system must be used. A limit is fixed on the simultaneous range-doppler resolution produce for pulsed amplitude modulated systems by the small time-bandwidth product. This limitation may be overcome by using random signal pulsed systems at the expense of increased complexity.

Pit Sampler: Some form of corroborative direct sampling is highly desirable to validate indirect methods particularly during early development stages. A pit sampler as mentioned in section 2, would be a suitable candidate. WASLENUK (1976) described a diver-operated pit sampler which with modification could be rig mounted. Continuous sampling might be achieved by using a pumped system similar to, or in conjunction with, the existing suspended pumped sampling system.

3. CONCLUSIONS

The dearth of instrumentation for the measurement of sediment transport is indicative of the problems involved. No completely new ideas have been generated in this report, nor do the suggested techniques fulfil all the design requirements.

Acoustic techniques are particularly attractive for bedload transport instruments, enabling measurements to be made very close to the sea bed and providing a continuous data output, without the sensors affecting the transport they are measuring.

The two acoustic techniques, (a) self-generated noise, and (b) doppler velocity and backscatter concentration measurement, are to a large extent complementary, each suited to a particular set of conditions, but both require laboratory and field development.

In Appendix A self-generated noise is considered in two ways. The first model provides information on which to base the use of the technique both as a threshold detector, and as a quantitative measurement of the bedload transport rate. However, the overall approach is a little naive and therefore its use should be limited to threshold considerations only. Calibrated field data on

ambient noise levels under conditions of no movement, in parallel with sediment noise data, are required in order to verify predictions and to enable a detailed specification to be produced.

In contrast, the second model exemplifies the difficulties involved in trying to produce quantitative data from the technique. Even for the simplified case given in Appendix A, the calculated rate of sediment transport is a function of at least five variables, which in addition to the measured sound pressure level are the size and mass of the particles, the position of the hydrophone, and the average acoustic power generated by a single collision between a moving and stationary particle (defined as SPL_{eq}).

By conducting laboratory experiments data may be obtained to determine SPL_{eq}/ u_b relationships for sand particles. Field measurements of the sound pressure level conducted in parallel with u_b determinations may then be capable of providing quantitative bedload measurements.

In practice, particle saltation, the complexity of areal movement and the depth of the bedload layer considerably complicate the situation. However, further investigation of the technique is warranted.

Appendix B discusses acoustic doppler and backscatter concentration measurement. Doppler techniques are capable of measuring the velocity of particle movement, both on the bed and in the water column. Bedload particle velocity data may be used in conjunction with the self-generated noise technique, while data from the 'saltation' layer and above may be combined with concentration measurements obtained from acoustic backscattering. Therefore by combined use of the techniques valuable experimental data on bedload transport should be forthcoming.

It is suggested in addition to the development of the indirect acoustic methods that a direct sampling method should also be investigated. This may be based on a pit sampler with pumped extraction of accumulated sand. Such a direct method would help to quickly fill the present instrumentation gap and also provide essential corroborative data for the indirect methods.

ACKNOWLEDGMENTS

I wish to express my appreciation for the help and advice provided by colleagues both inside and outside the Institute of Oceanographic Sciences. In particular to R L Soulsby, Drs K R Dyer, W R Parker and A D Heathershaw.

APPENDIX A

Self-generated noise

In this appendix bedload is considered from two viewpoints. Firstly, as a layer of saltating particles impacting on a stationary bed. Secondly, as material transported in "sheet flow", rolling in contact with the bed. Both these visualisations are idealised but may be represented by models that have been considered theoretically.

An analysis was presented by JOHNSON and MUIR (1969) for the saltation case, which is modified in this study in the light of recent data. The Einstein bedload equation expresses an equilibrium condition of particle exchange between the bedload transport layer and the bed. This implies that the number of particles deposited per unit time per unit bed area must be equal to the number of particles eroded per unit time and unit bed area.

Each particle with a given diameter, d , performs individual steps of constant length $k_1 d$ and is assumed to be deposited over an area $k_1 d$ long and of unit width. Observations indicate that k_1 appears to remain constant, independent of the flow condition, the transport rate and the bed composition. Different transport rates may be achieved by a change in the average time between jumps and in the thickness of the bedload transport layer.

Assuming a sediment of one uniform grain diameter, the number of particles deposited per unit time per unit bed area is given by:

$$\frac{6 j_b}{\pi k_1 d^4 \rho_s} \quad . \quad . \quad j_b = \begin{matrix} \text{mass per unit time} \\ \text{per unit width} \end{matrix} \quad (1)$$

According to the Hertz law of impact, GOLDSMITH (1960), the ratio of vibrational energy emitted by the collision of a moving sphere, velocity \bar{u}_b , with a stationary sphere, to the initial kinetic energy of the moving sphere is given by:

$$\frac{\bar{u}_b}{50 c_b} \quad c_b = \text{velocity of sound in the particle} \quad (2)$$

Assuming that this law is applicable to the impact at the termination of a saltation trajectory, the vibrational energy emitted by a single deposition is given by:

$$\left[\frac{\pi \rho_s d^3}{600 c_b} \right] \bar{u}_b^3 \quad (3)$$

Therefore the average vibrational energy emitted per unit time per unit bed area (acoustic intensity) caused by interparticle collision is:

$$I = \left[\frac{j_b}{100 k_1 d c_b} \right] \bar{u}_b^3 \quad (4)$$

Expected intensities for the bedload transport rates given in Table 3 (section 1.2) are shown in Table 4. (Experimental values for \bar{u}_b are taken from the flume studies of FERNANDEZ-LUQUE (1974) together with a value for $k_1 = 16$. This is a smaller value than that suggested by Einstein who quotes $k_1 \approx 100$ but is consistent with the \bar{u}_b data).

Sediment diameter $d, \mu m$	$u_* = 2.5 \text{ cms}^{-1}$	$u_* = 3.5 \text{ cms}^{-1}$	$u_* = 4.5 \text{ cms}^{-1}$
	$I \text{ Wm}^{-2}$	$I \text{ Wm}^{-2}$	$I \text{ Wm}^{-2}$
200	2.3×10^{-10}	1.0×10^{-8}	7.5×10^{-7}
500	8.9×10^{-11}	2.8×10^{-7}	4.7×10^{-6}
1000	3.57×10^{-11}	2.1×10^{-8}	7.6×10^{-5}

TABLE 4 Expected acoustic intensities generated by calculated bedload transport rates.

Expressing the data in Table 4 in equivalent pressure spectrum levels, $L_s, \text{ dBs}$ (assuming a measurement bandwidth of 3 kHz) yields the values in Table 5.

Sediment diameter $d, \mu m$	$u_* = 2.5 \text{ cms}^{-1}$	$u_* = 3.5 \text{ cms}^{-1}$	$u_* = 4.5 \text{ cms}^{-1}$
	$L_s \text{ dBs re } 1 \mu Pa$	$L_s \text{ dBs re } 1 \mu Pa$	$L_s \text{ dBs re } 1 \mu Pa$
200	+ 25.78	+ 84.22	+ 95.96
500	+ 17.43	+ 87.48	+ 112.02
1000	- 10.07	+ 65.36	+ 145.36

TABLE 5 Equivalent pressure spectrum levels for bedload transport.

In order to establish the range of conditions over which self-generated noise may be recognised, the data in Table 5 may be compared with background ambient noise levels. Figure 5 shows the Knudsen Curves for sea states 0 and 6 together with the thermal noise limit for an omnidirectional hydrophone. The shaded area represents the limits of data from Table 5. (The frequency/particle size relationship is extrapolated from data from MILLARD (1976)). Reference to Figure 5 suggests that thermal noise is most likely to limit the recognition of self-generated noise. This background level may be lowered by increasing the hydrophone directivity. Therefore, assuming that this analysis is valid, self-generated noise may be used to detect the motion of small quantities of sand in the marine environment and therefore as an indication of the threshold of movement. (Some care must be taken in the application of deep water spectrum

levels to the shallow water situation. Ambient noise levels in the coastal waters vary widely and a common working rule is to increase the deep water figure for a given sea state by +9 dBs, although this is likely to be an overestimate for frequencies greater than 50 kHz.)

In addition to the ambient background noise level, various specific interfering noise sources may be considered.

(i) Radiated ship noise

When deployed from an anchored ship (or from a beach) propeller cavitation and propulsion machinery noise are absent. In view of the frequencies involved, > 100 kHz, the additional ship noise sources are unlikely to cause marked interference. Some high frequency items of equipment, for example, echosounders, may be detected but should be easily recognised by their characteristic periodic signals.

(ii) Flow noise

The power spectrum of flow noise is flat at low frequencies, with a slope of -9 dB/octave at high frequencies. Consideration of the low flow velocities involved leads to the conclusion that flow noise will be of low amplitude and unlikely to mask sediment noise. Any effect may be reduced by using a relatively large hydrophone which averages out turbulent flow pressure fluctuations as a result of their small correlation distance.

(iii) Impact noise

Under flow conditions producing concurrent suspension, it is probable that suspended particles will impact on the hydrophone causing erroneous data. This effect may be reduced by housing the hydrophone in a cavity behind a diaphragm. This will also minimise the effect of flow noise and by suitable design may be used to increase hydrophone directivity. Therefore, it is considered that background noise sources will not seriously limit application of the technique, although for the detection of threshold movement an increase in hydrophone directivity is indicated.

The treatment of JOHNSON and MUIR is one possible relationship developed from a particular set of assumptions. An alternative treatment which is more applicable to the 'sheet flow' case is proposed by JONYS (1976). A modified form of Jonys method is given below and although the absolute values produced for the sound pressure level are not applicable to the sand size range, the effect of different parameters is illustrated.

In this model, it is assumed that all particles are spherical with a diameter, d , moving by rolling in a layer one diameter deep.

The rate of bedload transport in a width d may be given by:

$$j_{wb} = f \cdot m \quad (5)$$

f = frequency of passage of particles past a reference line
 m = particle mass

The mass of a particle is given by:

$$m = \rho_s \frac{\pi d^3}{6} \quad (6)$$

The passage frequency, f , depends on the average velocity of particles and for adjacent particles:

$$f = \frac{\bar{u}_b}{d}$$

Therefore

$$j_{wb} = \frac{m \bar{u}_b}{d} \quad (7)$$

Therefore the rate of bedload transport per unit width of channel is:

$$j_b = \frac{m \bar{u}_b}{d^2} = \frac{f \cdot m}{d} \quad (8)$$

To express the relationship between the number of collisions and the total sound pressure level at a point above the bed, a concentric arrangement of rings around the acoustic axis is employed.

The total number of particles in any circular ring i , located at a radius of N particle diameters from the acoustic axis may be estimated from:

$$N_i = 2\pi N \quad (9)$$

The total number of collisions per unit time in any ring i is given by:

$$F_i = f N_i \quad (10)$$

If more than one source contributes to the total sound pressure at a point, the total r.m.s. pressure for continuous sources is given by:

$$p = \sqrt{p_1^2 + \dots + p_n^2} \quad (11) \quad p_1 - p_n \text{ are the r.m.s. magnitudes of the individual source pressures}$$

When all the sources are equal the relationship may be expressed as:

$$SPL = SPL_x + 10 \log n \quad (12)$$

where SPL represents the sound pressure level in decibels produced by n sources each with an individual sound pressure level of SPL_x . Bedload transport produces pulses of sound and in order to consider the sound as at least quasi-steady the frequency of pulses must exceed a limiting frequency. JONYS (1976) determined experimentally that this limiting frequency may be taken as 50 Hz.

Equation (12) may be rewritten as:

$$SPL_{eq} = SPL - 10 \log F_i \quad (13)$$

where SPL_{eq} is the sound pressure level produced by one collision per second and F_i is the frequency of particle collision in Hz.

Assuming that SPL_{eq} is a function only of \bar{u}_b , and hence constant in a given flow situation, the sound pressure level contribution SPL_i produced by collisions in a ring i at a range r_i may be determined from:

$$SPL_i = SPL_{eq} + 10 \log F_i - 20 \log \frac{r_i}{r_0} \quad (14)$$

where r_0 is the vertical distance between the hydrophone and the bed.

Expressing equation (14) in terms of f and N_i :

$$SPL_i = SPL_{eq} + 20 \log r_0 + 10 \log \frac{f N_i}{r_i^2} \quad (15)$$

The total sound pressure level, SPL, is given by:

$$SPL = 10 \log \sum_{i=1}^{i=k} 10^{SPL_i/10} \quad (16)$$

where k = number of noise contributing rings, substituting from equation (15) into (16).

$$f = \frac{10^{\frac{SPL/10}{10}}}{r_0^2 \cdot 10^{\frac{SPL_{eq}/10}{10}} \sum_{i=1}^{i=k} \frac{N_i}{r_i^2}} \quad (17)$$

Substituting equation (17) into equation (8) produces:

$$J_b = \frac{m \cdot 10^{\frac{SPL/10}{10}}}{r_0^2 \cdot d \cdot 10^{\frac{SPL_{eq}/10}{10}} \sum_{i=1}^{i=k} \frac{N_i}{r_i^2}} \quad (18)$$

Comments on this method are given in the conclusions, section 3.0.

APPENDIX B

Acoustic Doppler

The characteristics of acoustic doppler systems are considered in two parts. Firstly the velocity and spatial resolution performance and secondly the acoustic scattering behaviour of sand particles in water. As stated in section 3 consideration is also given to application in the water column above the bed and not strictly to the bed alone.

Resolution of pulsed doppler sonar:

A block diagram for a basic pulsed doppler sonar is given in Figure 6. The operation is self-evident from Figure 7, which illustrates waveforms present at various sections of the block diagram.

Considering the performance of a basic pulsed system:

(a) Spatial resolution

Spatial resolution is a function of beam cross section and system bandwidth. Lateral resolution, ΔL , is approximately half the beam diameter, assuming a cylindrical geometry for transmission and reception by a single transducer. Axial resolution, ΔR , is inversely proportional to system bandwidth:

$$\Delta R = \frac{c}{2B} \quad (19) \quad \begin{array}{l} c = \text{velocity of sound} \\ B = \text{system bandwidth} \end{array}$$

Typically an axial resolution of 1cm may be obtained.

(b) Velocity resolution

Velocity resolution is determined by the shape of the doppler power spectrum. The ideal spectrum is a unit impulse located at frequency, f_D , given by:

$$f_D = \left(\frac{2Vf_0}{c} \right) \cos \theta \quad (20) \quad \begin{array}{l} f_D = \text{doppler frequency} \\ V = \text{velocity of scatterer} \\ f_0 = \text{ultrasonic carrier frequency} \\ \theta = \text{acute angle between flow axis and acoustic axis} \end{array}$$

A number of factors broaden the ideal; flow gradients, angular beamwidth

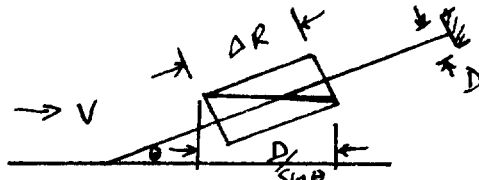
and finite transit time effects. Angular beamwidth effects may be minimised by careful transducer design, but transit time effects have a fundamental effect by limiting the time available for coherent processing.

The best doppler resolution that may be obtained is given by

$$\Delta f_D = \frac{1}{T_t} \quad (21) \quad T_t = \text{transit time}$$

The transit time for the configuration shown below is given by:

$$T_t = \frac{D}{2} \cdot \frac{1}{\sin \theta} \cdot \frac{1}{V} \cdot \frac{1}{2} \quad (22)$$



V = velocity of scattering centre

$\frac{D}{2}$ is used as an approximation to allow for a non-ideal distribution of energy across the beam diameter, while the additional factor of 0.5 accounts for variations in the backscattered signal as particles enter and leave the beam.

By differentiating (20),

$$\Delta V = \frac{\Delta f_D \cdot c}{2 f_0 \cos \theta} \quad (23)$$

from equations (21) and (22)

$$\Delta f_D = \frac{4 V \sin \theta}{D}$$

and with (23)

$$\frac{\Delta V}{V} = \left(\frac{2c}{D f_0} \right) \tan \theta \quad (24)$$

A $\frac{\Delta V}{V}$ of 0.05 may be obtained with the typical parameters given below:

$$\begin{aligned} f_0 &= 10 \text{ MHz} \\ \theta &= 45^\circ \\ D &= 0.6 \text{ cm} \\ c &= 1500 \text{ ms}^{-1} \end{aligned}$$

Equation (24) defines the fractional velocity resolution caused by a finite transit time. However velocity gradients across the active volume may produce an increase in the width of the doppler spectrum which is greater than the limitation imposed by the transit time effect.

Small time-bandwidth product restriction :

The range resolution and fractional velocity resolution are coupled by the small time-bandwidth product restriction. This places a limit on distortion in the modulation function which is produced if the scattering particle moves appreciably during the signal duration. The restriction is given by RIHACZEK (1969):

$$T \cdot B \leq \frac{0.1c}{V \cos \theta} \quad (25)$$

From (20)

$$B = \frac{c}{2\Delta R} \quad (26) \quad \Delta R = \text{axial resolution}$$

Let

$$T = \frac{D}{4V \sin \theta} \quad (27)$$

Combining equations (26) and (27)

$$T \cdot B = \frac{cD}{8V \sin \theta \Delta R} \quad (28)$$

Therefore

$$\Delta R \geq \frac{1.25 D}{\tan \theta}$$

Ambiguities

Range Ambiguity:

To avoid range ambiguity the pulse repetition frequency, f_r , is given by:

$$f_r < \frac{c}{2R} \quad (29) \quad R = \text{one way range}$$

Velocity Ambiguity:

To avoid velocity ambiguity, f_r , is given by

$$f_r > 2f_D \quad (30)$$

Equation (30) may be combined with (20) to give:

$$f_D > \frac{c^2}{8RV_{\max} \cos \theta} \quad (31)$$

or $V R_{\max} < \frac{c^2}{8 f_0}$, showing that the product of maximum velocity and range are limited. For example, a system operating at 10 MHz has a $V \cdot R_{\max}$ of $281 \text{ cm}^2 \text{ s}^{-1}$.

Random Signal System

The range ambiguity limitation may be overcome by using a random signal system, in which pulsed bursts of random noise are transmitted. The range resolution for a random signal system is the same as for a conventional pulsed system, ie

$$\Delta R = \frac{c}{2B}$$

The random signal system range resolution depends only on the transmitted bandwidth, and not on the output pulse length. The ability of the random signal system to resolve targets at the same range but with different velocities depends primarily on the bandwidth of the output filter after the correlator. The velocity resolution is given by:

$$\Delta V = \frac{cW}{2f_0} \quad W = \text{filter bandwidth}$$

Therefore for a random signal system ΔV and ΔR are independent and are only limited by bandwidth considerations. Another important characteristic of random systems is the larger output signal/noise ratio. The duty factor may be kept large allowing high average power to be transmitted without resorting to the short high peak power pulses of a conventional pulsed system. A schematic diagram of a random signal system is given in Figure 8.

Flow measurement with a random signal system.

If the transmitted noise signal has an amplitude $x(t)$ the received echo from a single moving target is of form $Ax[(1+\alpha)t - \tau_s]$ where A is the randomly varying scattering cross section, τ_s is the signal time of flight and $\alpha = \frac{v \cos \theta}{c}$

The time average of the correlator output $Z(t)$ is proportional to:

$$\bar{A} R(\tau) [\alpha t - (\tau_s - \tau_d)]$$

\bar{A} = time average scattering cross section
 τ_d = time delay of reference
 $R(\tau)$ = autocorrelation function of τ_s for variable τ_d

For a transmitted spectral density of $S(f) = \frac{2B}{[B^2 + [2\pi(f-f_0)]^2]}$

the time average correlator output will be:

$$Z(t) = \bar{A} e^{-B|\Delta t - (\tau_s - \tau_d)|} \cos 2\pi f_0 [\Delta t - (\tau_s - \tau_d)]$$

Therefore for a single target in the 'range cell', ie where $\tau_s \approx \tau_d$, an output of the form $e^{-B|\Delta t|} \cos 2\pi f_0 \Delta t$ is obtained.

The spectrum of this output consists of a compressed version of the transmitted spectrum, centred around the doppler shift frequency:

$$S_R(f) = \frac{2\Delta B}{(\Delta B)^2 + 2\pi(f - \Delta f_0)^2}$$

The fact that a single particle leads to a finite width doppler spectrum is due to the limited time spent in the range cell, and is identical to transit time broadening in conventional pulsed systems.

If a distribution of scatterers travelling at constant velocity pass through the range cell at random time intervals determined by a Poisson distribution, the correlator output spectrum is unchanged from that of a single scatterer. Therefore the relationship between the doppler output spectrum and the transmitted spectrum is the same whether the transmitted signal is a burst of RF or a stationary random signal.

However, the random systems have the advantages of a higher signal to noise ratio, lower peak output power and no range ambiguity, but these have to be weighed against increased system complexity.

Measurement of concentration

Particles undergoing bedload transport fall into two distinct categories when concentration is to be measured by acoustic techniques. These are the same as in Appendix A, ie those undergoing 'sheet' transport in contact with the bed and those transported by saltation.

For sheet flow a surface/volume scattering mechanism operates. Although at normal incidence experimental measurements indicate correlation between the acoustic reflection coefficient and porosity (FAAS, (1959), AKAL (1972)), such correlations are not applicable to this situation and technique. However, doppler measurement of \bar{u}_b , the mean bedload particle velocity may be applied in conjunction with the self-generated noise technique mentioned in Appendix A.

Within the 'saltation layer' and above, a volume scattering situation exists. There are two signal processing techniques that may be used for estimating the spatial density of scatterers from acoustic returns. When the density of

scatterers is low and echoes do not overlap temporally, the scattering density may be estimated by echo counting. When the density is high, the total scattered energy is a measure of the spatial density and echo integration is more appropriate.

The errors created by echo overlap have been evaluated by EHRENBERG (1972) and are of the general form illustrated in Figure 9. At low densities both processing techniques exhibit errors due to variance in the scatterer distribution. As the density increases both processors produce fewer errors until echo overlap begins to significantly bias the output of the echo counter at densities greater than 0.1 scatterers per unit volume. This bias becomes unacceptably large at densities of greater than 1 scatterer per pulse volume and it is necessary either to decrease the measurement volume or resort to the echo integrator.

The number density of particles present in a typical measurement volume (0.5 ml) are given in Table 6.

c_{ppm} \ d μm	250	500	1000
3	0.07	0.01	0.001
30	0.7	0.09	0.01
300	7.0	0.9	0.11
4000	90	12	1.45

Taken from
SOULSBY, 1977

TABLE 6 Number of grains in 0.5 ml.

The concentrations chosen in Table 6 are low, typically the range 3.0 - 5000 ppm will be obtained at approximately ten centimetres above the bed. Within the 'saltation layer' concentrations will be considerably higher and will tend to occur with the smaller size grains. 'Sheet flow' is more likely with the larger size material. Therefore, echo integration is the applicable technique near the bed.

Echo Integration and Reverberation Theory

Various simplifying assumptions are made in the theory outlined below:

- (1) Straight line propagation
- (2) Random homogeneous distribution of scatterers
- (3) Density of scatterers is large in elemental volume dV or area dA
- (4) Pulse duration is short enough for propagation effects over range extension of elemental volume as area to be neglected.
- (5) No multiple scattering.

Considering volume reverberation:

The equivalent plane wave reverberation level, RL, is defined by URICK (1967) as:

$$RL = 10 \log_{10} \left[\frac{I_0}{r^4} S_v \int_V b^2(\theta, \phi) dV \right]$$

where I_0 = axial output intensity at unit distance

r = range

$10 \log_{10} S_v = S_v$ = backscattering strength

$b(\theta, \phi)$ = beam pattern function

The elemental volume dV may be considered as an infinitesimal cylinder with end face areas $r^2 d\Omega$ and length $\frac{c\tau}{2}$ therefore:

$$dV = r^2 \frac{c\tau}{2} d\Omega$$

The integral $\int b^2(\theta, \phi)$ may be converted into the equivalent beamwidth, Φ

where $\int_0^{4\pi} b^2(\theta, \phi) d\Omega = \Phi$

The equivalent plane wave volume reverberation level, RL_v , may then be written as:

$$RL_v = 10 \log_{10} \left[\frac{I_0}{r^4} S_v \frac{c\tau}{2} \Phi r^2 \right]$$

or

$$RL_v = SL - 40 \log_{10} r + S_v + 10 \log_{10} v \quad v = \frac{c\tau}{2} \Phi r^2$$

The backscattering strength S_v is dependent on the type and density of scatterers, and may be expressed as $\rho_v \sigma_v$, where ρ_v is the particle density in mass per unit volume and σ_v is the mean backscattering cross section per unit mass of particles.

The backscattering cross section characteristics of a solid sphere shows three regions controlled by the acoustic wavelength/sphere radius ratio, normally given by $ka = \frac{2\pi a}{\lambda}$. Figure 10 shows the ratio of the backscattering cross section to the geometric cross section as a function of ka .

Constraints forced on the operating frequency by bandwidth requirements and velocity ambiguities require frequencies in the megahertz range. This precludes operation in the Rayleigh region. The fluctuations that occur in the diffraction region are to be avoided, and consequently operation in the geometric region is required.

Table 7 gives the ka values for a range of frequencies and scattering particle diameters.

f MHz \ d μ m	100	250	500	1000
1	0.21	1.03	1.05	2.1
5	1.05	2.6	5.25	10.45
10	2.1	5.25	10.5	21
15	3.14	7.85	15.7	31.4

TABLE 7. ka values for sand particles

Amplitude fluctuations at the edge of the diffraction region effectively die out for $ka > 5$, therefore for particles with a diameter $> 200 \mu\text{m}$ frequency of 10 MHz is suitable.

In practice the situation is more complex because the propagation of high frequency acoustic energy is modified by attenuation and non-homogeneities in the propagation path. At megahertz frequencies the attenuation due to absorption in 'clean' sea water is approximately 3.2 dB/m/MHz which is acceptable for the operating ranges required for bedload instrumentation. However attenuation due to viscous absorption increases if fine particulate material is present. Figure 11 shows the typical shape of the attenuation curve. As a consequence application of high frequency doppler techniques will be limited to use in water with a low concentration of mud and silt.

Summary to the acoustic measurement of particle concentration

1. Operating frequencies will be of the order 5 - 10 MHz
2. Measurement of the concentration of material in contact with the bed is not feasible.
3. Echo integration techniques have to be applied, and knowledge of various sonar parameters is also required. EHRENBERG (1972, 1974a and 1974b) discusses these factors in detail.
4. Information on the scattering behaviour of sand in water is necessary. Studies by OUTSUKI (1978), provide preliminary data and further information may be obtained by laboratory investigation.

Tentative Design

A preliminary specification giving a feel for the design parameters involved is given below:

Transducer diameter D = 0.8 cm
Acute angle to flow θ = 45°
Operational frequency f_0 = 10 MHz
Height of transducer = 15 cms
Maximum particle velocity, V, = 30 cms^{-1}

The system given above would have the following resolutions:

Fractional velocity resolution $\frac{\Delta v}{V}$ = 3.8×10^{-2}
Range resolution (small TB limit) = 1.0 cm

REFERENCES

- Ackers, P and White, W R (1965) "Sediment Transport: New Approach and Analysis"
J. Hydraulics Div. ASCE 99 (HY11): 2041-2061.
- Akal, T (1972). "The Relationships between the Physical Properties of Underwater Sediments that affect Bottom Reflection". Marine Geology 13: 251-266.
- Bagnold, R A (1966) "An Approach to the Sediment Transport Problem from General Physics". US Geol. Survey, Prof. Paper 422-J.
- Bedeus, K and Ivisics, L (1963). "Observation of the noise of the bed load"
Proc. Internat. Assoc. Sci. Hydrology. Publ. No 65, p.384.
- Bhattacharya, P.K. et al (1969). "An Electro-Optical Probe for Measurement of Suspended Sediment Concentration". Proc. Congr. 13th IAHR 2: 241-250.
- Brenninkmeyer, S J (1976). "In Situ Measurements of Rapidly Fluctuating High Sediment Concentrations". Marine Geology 20, 117-128.
- Du Boys, M P (1879). "Le Rhône et les Rivières à lit affouillable". Mem. et Doc, Annales des Pont et Chaussées, ser. 5, vol XVIII
- Einstein, H A (1950). "The Bed-load Function for Sediment Transportation in Open Channel Flows". Tech Bull. No. 1026. Sept 1950. US Dept of Agriculture.
- Ehrenberg, J E (1972). "Acoustic Techniques for estimating fish abundance"
IEEE Transactions GE-10: 138-145.
- Ehrenberg, J E (1974a) "Two applications for a dual beam transducer in hydro-acoustic fish assessment systems". Proc. 1974 IEEE Conf. Engr. Ocean Environ. : 152-155.
- Ehrenberg, J E (1974b) "Recursive algorithm for estimating the spatial density of acoustic point scatterers". J. Acoust. Soc. Am. 56 (2): 542-547 1974.
- Faas, R (1969). "Reflectivity and Porosity". Geophysics 34(4): 546-553
- Federal Inter-Agency River Basin Committee (1940). A Study of method used in measurement and analysis of sediment loads in streams.
Report No 2, 57 pp.
- Fernandez-Luque, R (1974). "Bed load transport along an Inclined Plane".
Euromech 48: Transport erosion and deposition of sediment in turbulent streams, 22-24 Aug. 1974, pp 26-28.

- Francis, J R D (1973). "Experiments on the motion of solitary grains along the bed of a water stream". Proc R Soc Lond A332; 443-471.
- Goldsmith, W (1960). "Impact - the theory and physical behaviour of colliding solids". Arnold, London.
- Graf, W H (1971). "Hydraulics of Sediment Transport". McGraw Hill
- Hubbell, D W (1964). "Apparatus and Techniques for Measuring Bed-Load". US Geol. Survey, Water Supply Paper 1748.
- Johnson, P and Muir, T C (1969). "Acoustic Detection of Sediment Movement". Journal of Hydraulic Research. 7 (4): 520-540.
- Jonys, C K (1976). "Acoustic Measurement of Sediment Transport". Scientific Series No 66. Inland Waters Directorate CCIW Branch. Burlington, Ontario
- Kachel, N B and Sternberg, R W (1971). "Transport of bedload as ripples during an ebb current". Marine Geology 19: 229-244.
- Millard, N W (1976). "Noise Generated by moving sediments". Proc. of IoA Underwater Acoustics Group Conf, Portland. 1976. Session 3.5.
- Millard, N W (1976b). Private communication
- Outsuki, S (1978). "Measuring method of target strength of sands suspended in water". Bull. Res. Labs. PME (37): 7-15.
- Raudkivi, A J (1967). "Loose Boundary Hydraulics" Pergamon Press.
- Richardson, E V et al (1961). "Sonic depth sounders for laboratory and field use". US Geol. Survey Circular 450, 7p.
- Rikaczek, A W (1969). "Principles of High Resolution Radar". McGraw Hill
- Shields, A. (1936). "Anwendung des Ahnlichkeits mechanik and Turbulenzforschung auf die Geschrebebewegung". Mitteil. Preuss. Versuchsanst. Wasser, Erd. Schiffsbau Berlin, No 26.
- Soulsby, R L (1977). "Sensors for the Measurement of Sand in Suspension" Institute of Oceanographic Sciences, Report No 27.
- Sternberg, R W (1972). "Predicting Initial Motion and Bedload Transport of Sediment Particles in the Shallow Marine Environment". Ch 3: Shelf Sediment Transport, Ed. Swift Duane and Pilkey. Dowden Hutchinson and Ross
- Urlick, R J (1967). "Principles of Underwater Sound" McGraw Hill
- Waslenchuk (1976) New Diver Operated Bedford Sampler
J. Hydraulics Div. ASCE 102 (HY6): 747-757.

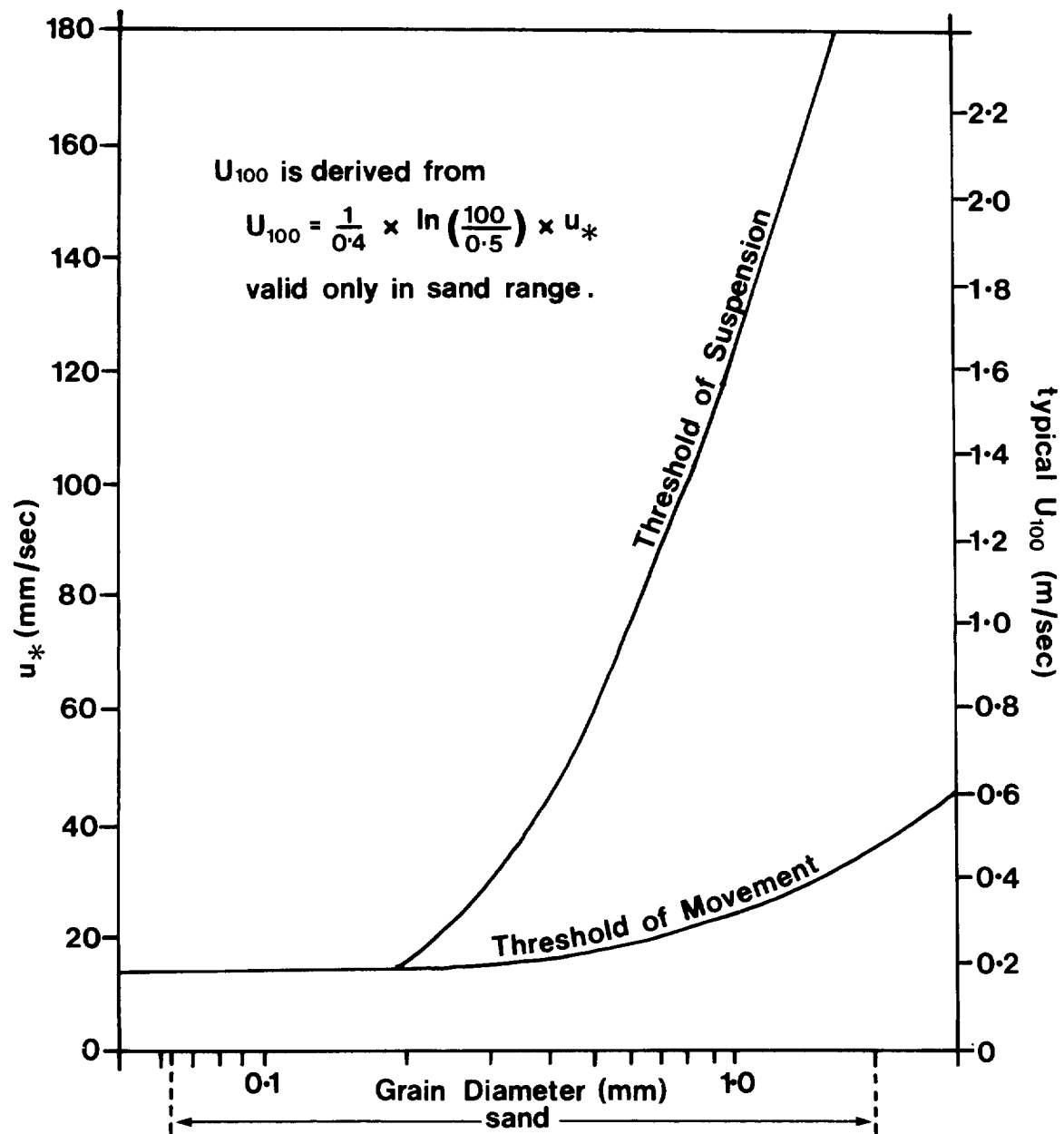


Figure 1.

Threshold values of shear velocity for bed-load movement, and for suspension. Values for U_{100} shown assume a logarithmic velocity with a roughness length of 5mm.

(After Soulsby 1977)

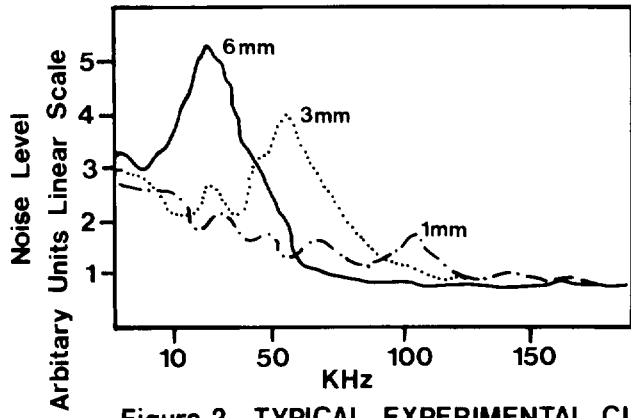


Figure 2. TYPICAL EXPERIMENTAL CURVES
(After Millard 1976)

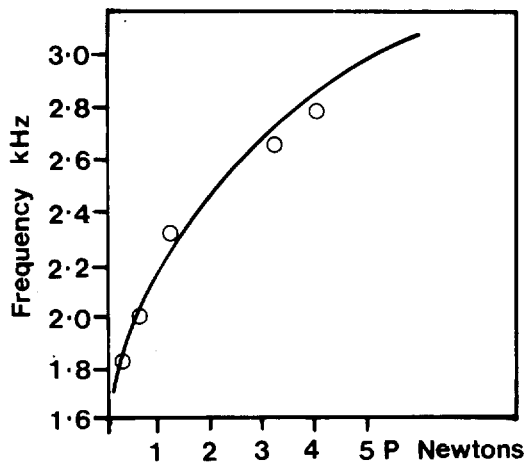


Figure 3. THEORETICAL LINE FOR
2.7cm SPHERES WITH EXPERIMENTAL
RESULTS SHOWN ○

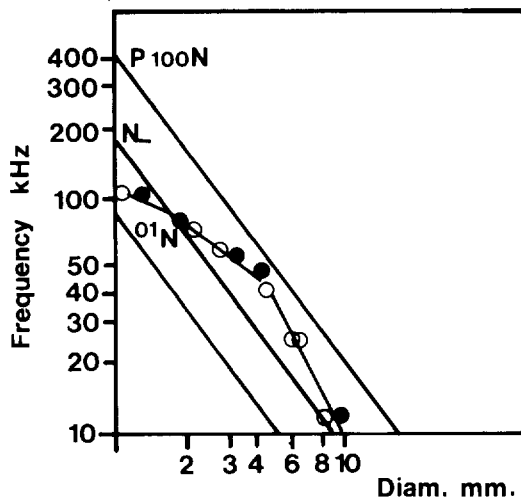


Figure 4.

- Glass spheres
- Coarse sand or shingle

(After Millard 1976)

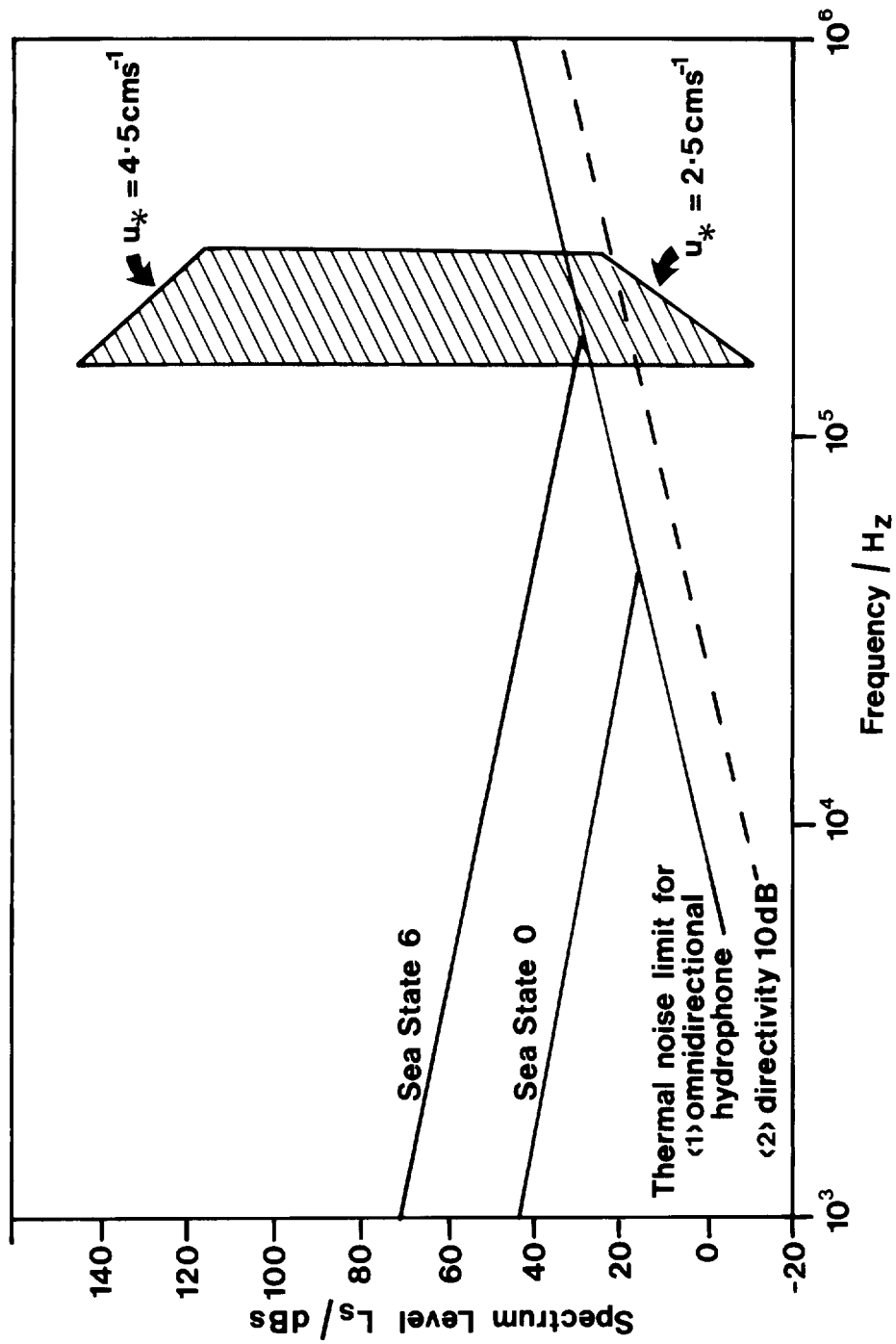


Figure 5. AMBIENT NOISE LEVELS TOGETHER WITH SUPERIMPOSED SELF GENERATED NOISE PREDICTIONS

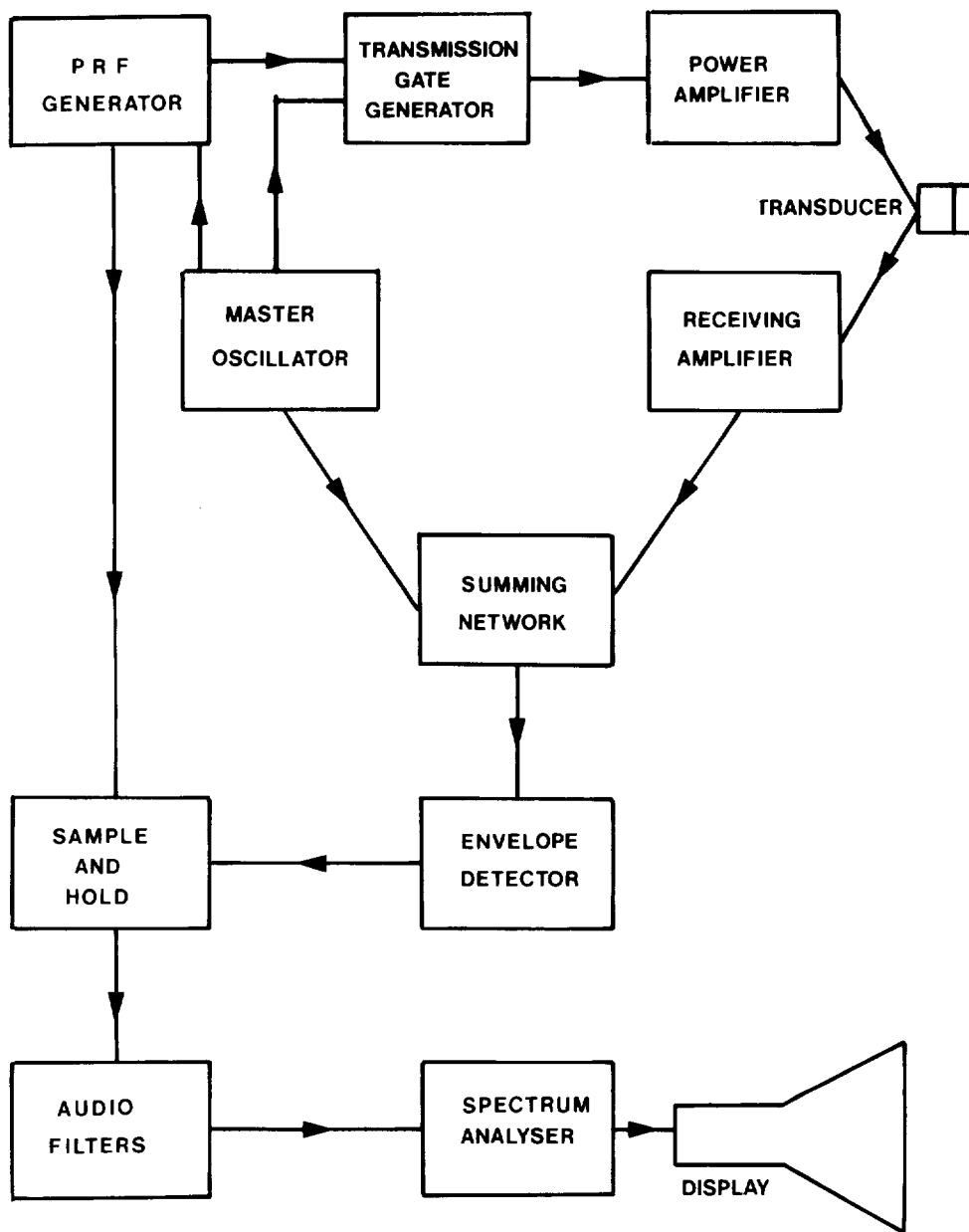


Figure 6. BLOCK DIAGRAM OF A PULSED-DOPPLER SYSTEM

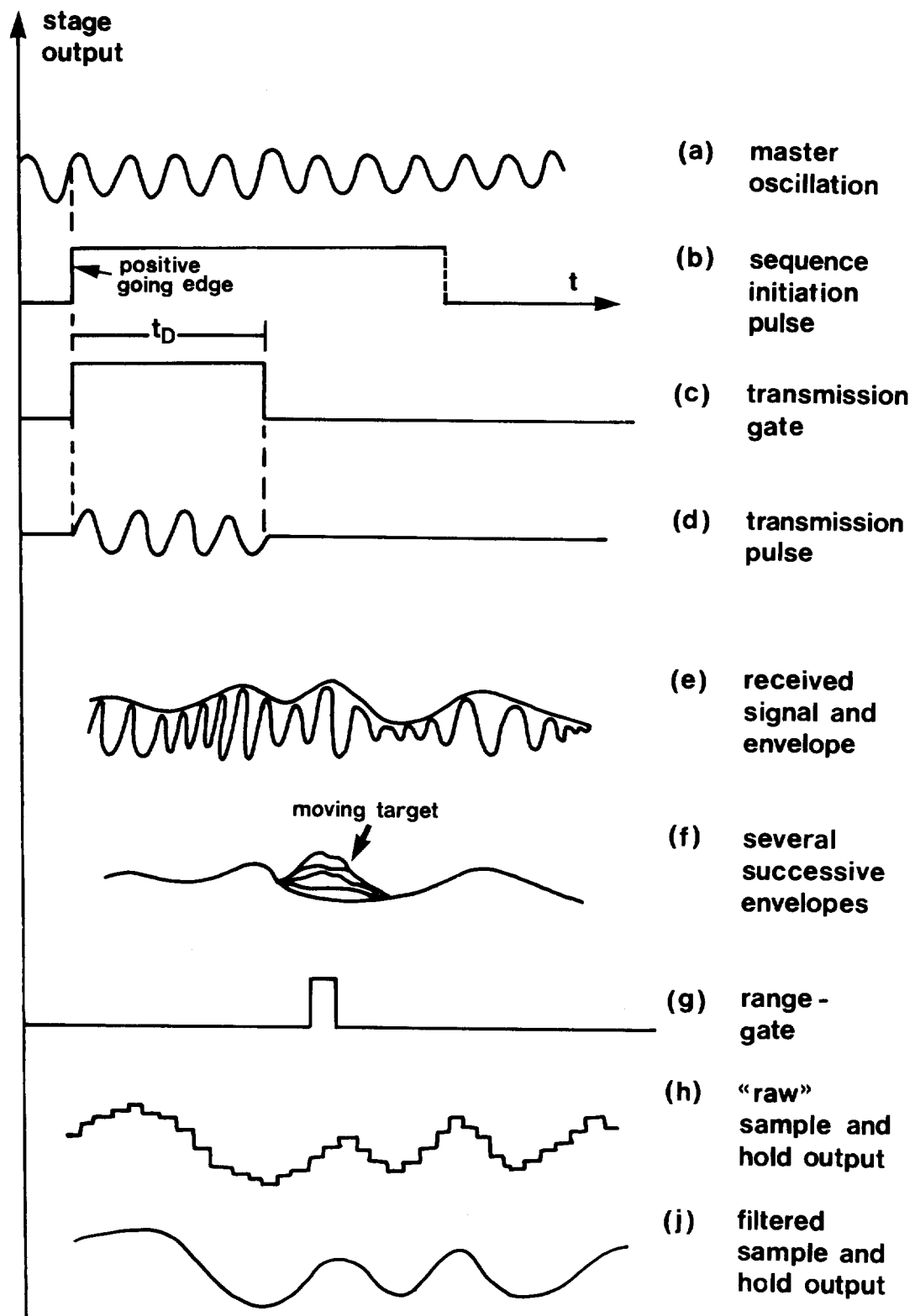


Figure 7. PULSE-DOPPLER WAVEFORMS

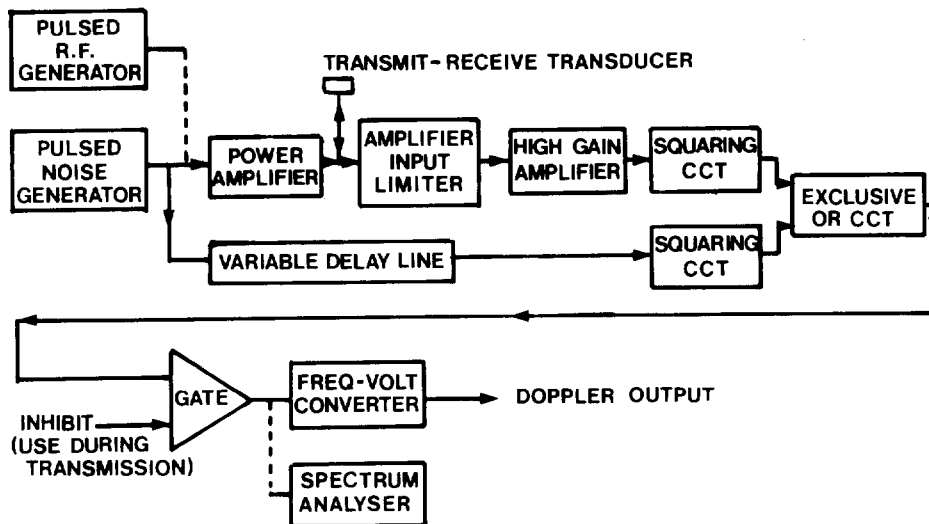


FIG. 8 SINGLE-TRANSDUCER RANDOM-SIGNAL FLOW MEASUREMENT SYSTEM.

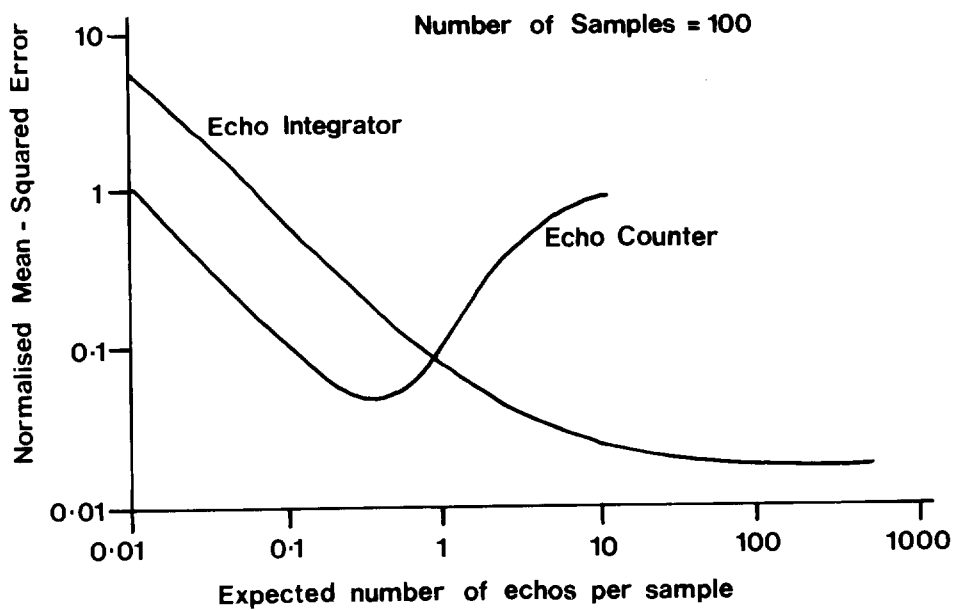


Figure 9. NORMALISED MEAN SQUARED ERRORS OF SIGNAL ESTIMATORS (After Ehrenberg 1974)

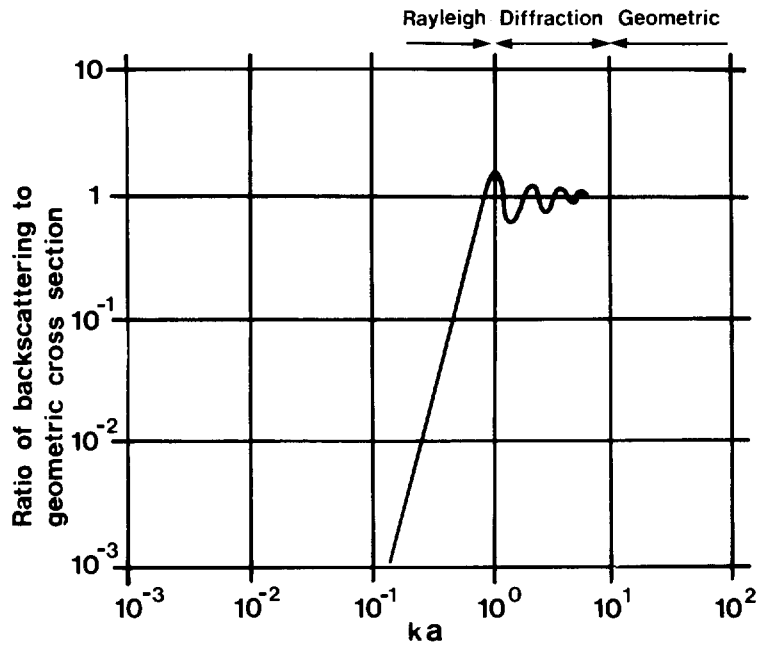


Figure 10. RATIO OF ACOUSTIC TO GEOMETRIC CROSS SECTION OF A FIXED RIGID SPHERE OF RADIUS a

(After Urick 1967)

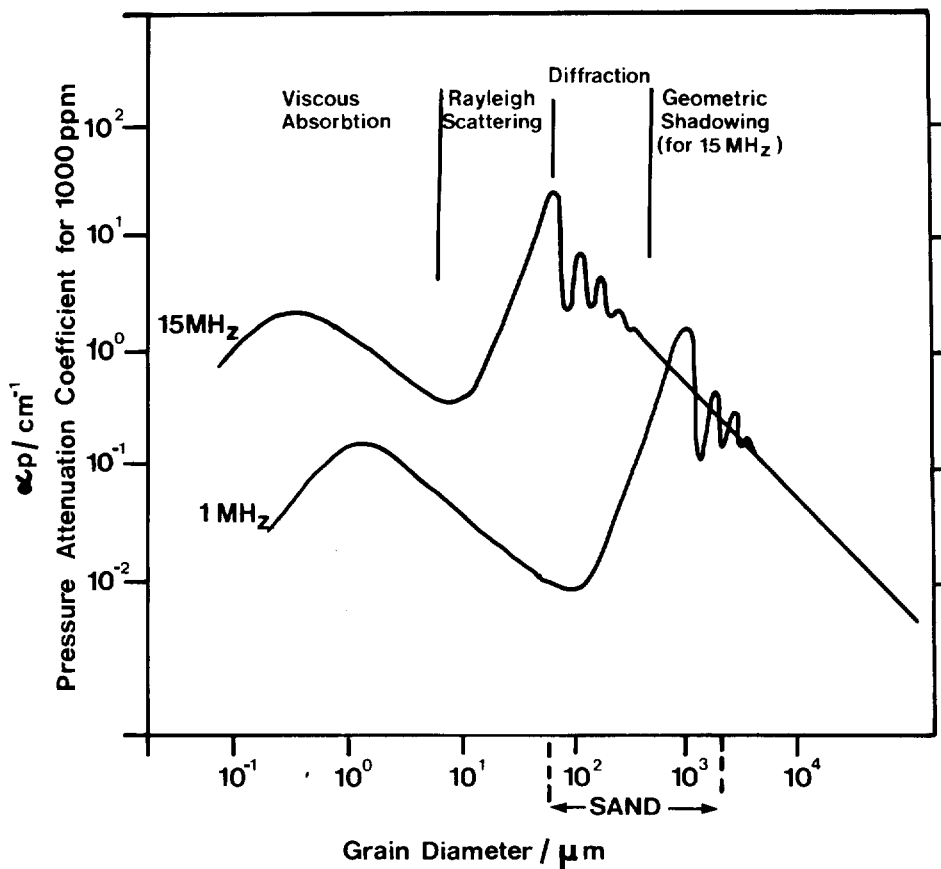


Figure 11. PRESSURE ATTENUATION COEFFICIENT α_p FOR SOUND PASSING THROUGH 1000 ppm SUSPENSION

(After Soulsby 1977)